

Synthesis and Dynamic Behaviour of Zwitterionic $[(\eta^6\text{-C}_6\text{H}_5\text{-BPh}_3)(\text{coe})_2]$ ($\text{M} = \text{Rh}, \text{Ir}$) Cyclooctene Complexes

Jesús J. Pérez-Torrente,* Marta Angoy, Daniel Gómez-Bautista, Adrián Palacios, M. Victoria Jiménez, F. Javier Modrego, Ricardo Castarlenas,[§] Fernando J. Lahoz and Luis A. Oro

5

The synthesis and structural characterization of zwitterionic $[(\eta^6\text{-C}_6\text{H}_5\text{-BPh}_3)\text{M}(\text{coe})_2]$ ($\text{M} = \text{Rh}, \text{Ir}$) cyclooctene complexes is described. Both complexes exhibit an unusual *exo-endo* conformation of both cyclooctene ligands in the solid state. However, an equilibrium between the *endo-endo* and *exo-endo* rotational isomers arising from the hindered rotation about the metal-cyclooctene bond is observed in solution. Rotational barriers of around $65 \text{ kJ}\cdot\text{mol}^{-1}$ (Rh) and $84 \text{ kJ}\cdot\text{mol}^{-1}$ (Ir) have been determined by 2D EXSY NMR spectroscopy. The rotation process has also been studied by DFT calculations showing that the dynamic behaviour is a consequence of the oscillation of the cyclooctene ligands about the metal-olefin bond instead of completing a full rotation.

15 Introduction

Zwitterionic transition metal complexes composed of a cationic metal fragment and a negatively charged ancillary ligand within an overall neutral molecular framework have attracted considerable attention.¹ Usually, these complexes exhibit the broad solubility and solvent tolerance of neutral species while maintaining the reactivity pattern of related cationic complexes, which have a limited solubility.²

Tetraphenylborate, BPh_4^- , has been largely utilized as a weakly coordinating anion in transition metal-based chemistry resulting in the formation of discrete ionic metal complexes.³ However, the coordination ability of tetraphenylborate through the phenyl rings provide access to species featuring strong metal- η^6 -arene interactions which remain as the most widely explored zwitterionic transition metal complexes.⁴ This is particularly true for rhodium chemistry where a range of zwitterionic rhodium(I) tetraphenylborate complexes containing both mono- and bidentate ligands such as $[(\eta^6\text{-C}_6\text{H}_5\text{-BPh}_3)\text{RhL}_2]$ ($\text{L} = \text{PR}_3$,⁵ P(OR)_3 ,⁶ ethylene⁷) and $[(\eta^6\text{-C}_6\text{H}_5\text{-BPh}_3)\text{Rh(L-L)}]$ ($\text{L-L} = \text{diene}$,⁸ P-P ,⁹ N-N^{10}), have been prepared.

Of particular relevance are the diene complexes that have found application as catalyst precursors for useful synthetic transformations. Alper *et al.* demonstrated the ability of $[(\eta^6\text{-C}_6\text{H}_5\text{-BPh}_3)\text{Rh}(\text{cod})]$ ($\text{cod} = 1,5\text{-cyclooctadiene}$) to catalyze a diversity of carbonylation reactions.¹¹ More recently, this compound has also been shown to promote the arylation of several unsaturated compounds using tetraarylborate as phenyl source.¹² On the other hand, complexes $[(\eta^6\text{-C}_6\text{H}_5\text{-BPh}_3)\text{Rh}(\text{diene})]$ ($\text{diene} = \text{cod}, \text{nbd}, \text{tfb}$) have been proven to be efficient initiators for the polymerization of monosubstituted acetylenes.¹³ It has been found that the π -acidity of the diene ligand strongly influences the catalytic activity.¹⁴ In fact, the nbd and tfb zwitterionic complexes ($\text{nbd} = 2,5\text{-norbornadiene}$, $\text{tfb} = \text{tetrafluorobenzobarelene}$) have shown an outstanding catalytic activity allowing for the preparation of highly stereoregular poly(phenylacetylene)s.¹⁵

Our research interest has been recently focused on the synthesis

and catalytic applications of transition metal complexes containing heteroditopic ligands of hemilabile character that incorporate strong electron donors, such as phosphines and carbenes.¹⁶ We have shown the potential of flexible hemilabile functionalized phosphine ligands of the type $\text{Ph}_2\text{P}(\text{CH}_2)_n\text{Z}$ ($\text{Z} = \text{OR}, \text{NR}_2$) for the design of efficient rhodium catalysts for the stereoregular polymerization of phenylacetylene,¹⁷ and the regioselective anti-Markovnikov oxidative amination of alkenes.¹⁸ In this context, we envisage the usefulness of the zwitterionic complex $[(\eta^6\text{-C}_6\text{H}_5\text{-BPh}_3)\text{Rh}(\text{coe})_2]$ for the synthesis of diene-free catalyst precursors by replacement of the labile cyclooctene ligands by functionalized phosphine ligands.¹⁹

We report herein on the synthesis and characterization of zwitterionic $[(\eta^6\text{-C}_6\text{H}_5\text{-BPh}_3)\text{M}(\text{coe})_2]$ ($\text{M} = \text{Rh}, \text{Ir}$) complexes. Much to our surprise, we have found that both compounds exhibit a dynamic behaviour associated to restricted rotation of the *coe* ligands. Olefin complexes are typically dynamic in nature and, as matter of fact, the propeller-like rotation of bound ethylene about the metal-olefin bond is a well-known process supported by abundant experimental work besides spectroscopic and theoretical studies.^{20,21} However, this phenomenon is much less common for cyclooctene complexes²² and, to our best knowledge, has never been reported for bis-cyclooctene complexes.

Results and discussion

Compound $[(\eta^6\text{-C}_6\text{H}_5\text{-BPh}_3)\text{Rh}(\text{coe})_2]$ (**1**) was prepared by reaction of $[\text{Rh}(\mu\text{-Cl})(\text{coe})_2]_2$ with a 10% excess of NaBPh_4 over the stoichiometric amount (2 equiv) in methanol and isolated as a pale yellow solid in excellent yield. The compound was fully characterized by elemental analysis, mass spectrometry and multinuclear NMR spectroscopy. In addition, the zwitterionic character of **1** was further confirmed by an X-ray diffraction study, which showed the η^6 -arene coordination of the tetraphenylborate anion (Figure 1a).

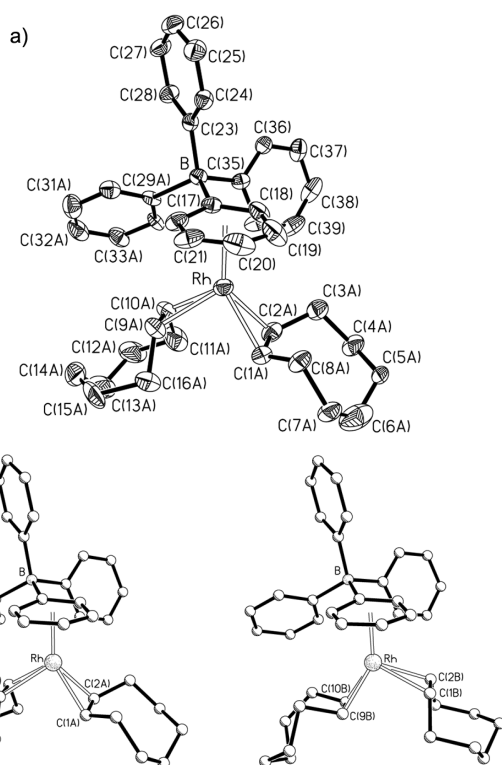


Figure 1. a) Molecular structure of $[(\eta^6\text{-C}_6\text{H}_5\text{-BPh}_3)\text{Rh}(\text{coe})_2]$ (**1**). Only the two disordered cyclooctene molecules with higher occupancy have been represented (C(1A) to C(16A)). b) Two schematic molecular structures of **1** showing the disorder of the cyclooctene molecules. The model with higher occupancy (A-labelled, left), with an *endo* conformation for C(1A) and C(2A), and *exo* for C(9A) and C(10A). On the right, the less abundant disordered complex (B-labelled) with an alternate conformation of both olefins.

The metal complex results to show a half-sandwich structure with a η^6 -coordination of one of the phenyl groups of the BPh_4^- anion and two η^2 -cyclooctene ligands, linked through their olefinic bonds, completing the metal environment. Both coordinated olefins exhibit clear static disorder and have been modeled on the base of two molecules with complementary occupancy factors (0.678 and 0.322(4)). As it is shown in Figure 1b, the cyclooctene disorder determined in the crystal involves a formal 180° -rotation of the double bonds about the rhodium-olefin vector, together with a modification of the G-Rh-M bond angle, from a mean value of $143.23(12)^\circ$ for the *endo* disposition to a value of $118.97(11)^\circ$ in the case of the *exo* conformation. Table 1 collects selected bond distances angles for **1**, stating data only for the two disordered cyclooctene molecules with higher occupancy.

Table 1. Selected bond distances (\AA) and angles ($^\circ$) for the zwitterionic complexes $[(\eta^6\text{-C}_6\text{H}_5\text{-BPh}_3)\text{M}(\text{coe})_2]$ ($\text{M} = \text{Rh}$ (**1**), Ir (**2**)).

	(1)	(2)	(1)	(2)
Rh/Ir-G*	1.8314(13)	1.806(2)	Rh/Ir-M(1)*	2.057(3)
Rh/Ir-C(17)	2.410(3)	2.401(5)	Rh/Ir-C(1)	2.153(4)
Rh/Ir-C(18)	2.337(3)	2.241(5)	Rh/Ir-C(2)	2.192(4)
Rh/Ir-C(19)	2.261(3)	2.280(5)	Rh/Ir-M(2)*	2.135(3)
Rh/Ir-C(20)	2.322(3)	2.304(5)	Rh/Ir-C(9)	2.216(4)
Rh/Ir-C(21)	2.288(3)	2.233(6)	Rh/Ir-C(10)	2.275(5)
Rh/Ir-C(22)	2.250(3)	2.312(6)	C(1)-C(2)	1.398(5)
G-Rh/Ir-	141.45(9)	139.61(15)	G-Rh/Ir-	123.49(10)
M(1)*			M(2)*	
M(1)-Rh/Ir-	94.93(13)	97.4(3)		
M(2)*				

* Only geometrical parameters for the most abundant disordered cyclooctene molecules are stated. *G represents the centroid of the C(17)-C(22) η^6 -coordinated phenyl ring; M(1), and M(2) represent the midpoints of the C(1)-C(2) and C(9)-C(10) olefinic double bonds.

Although the heavy disorder of the cyclooctene molecules (and also those of a phenyl group and the solvent molecule) precludes obtaining precise structural parameters, from the data determined for **1** a clear asymmetry in the η^6 -arene coordination is evident (Rh-C(arene) distances in the range 2.250-2.410(3) \AA), most probable as a consequence of the different dispositions of the cyclooctene ligands on the other side of the metal coordination sphere.

The most striking feature of the molecular structure of **1** is the different relative disposition of both cyclooctene ligands. The $=\text{CH}$ protons of a coe ligand are directed towards the Rh-arene fragment (*exo* conformation) whereas those of the second coe ligand point away this fragment (*endo* conformation). Interestingly, nearly all the " $\text{M}(\text{coe})_2$ " rhodium(I) and iridium(I) complexes structurally characterized, including both square planar²³ and 18 electron complexes having arene or polycyclic aromatic hydrocarbons,²⁴ exhibit an *endo-endo* conformation, with the notable exception of a heterobimetallic Pd-Ir complex featuring a functionalized 2-indenylidene pincer ligand that displays an $\text{Ir}(\text{coe})_2$ metal fragment with an *exo-endo* disposition.²⁵

The ^1H NMR spectrum of **1** in CD_2Cl_2 at room temperature showed featureless resonances for the protons of the coordinated phenyl ring, which suggests some kind of fluxional behaviour. Unexpectedly, the spectrum obtained at 253 K showed two sets of high-field shifted sharp resonances corresponding to coordinated phenyl rings, which are indicative of the presence of two different η^6 -arene species in a 1:1 ratio. Both species were also observed in the $^{13}\text{C}\{^1\text{H}\}$ NMR spectrum that displays two sets of three upfield-shifted doublet resonances for the CH carbons of the coordinated phenyl ring due to coupling with rhodium. The ^1H - ^1H NOESY spectrum shows strong exchange cross-peaks between the *ortho*, *meta* and *para* protons, respectively, besides of weak NOE cross-peaks, which indicate that both species interconvert in solution (Figure 2a). The exchange process is also observed for the $=\text{CH}$ resonances of the cyclooctene ligands (Figure 2b) which strongly suggests the presence of two rotamers arising from the hindered rotation about the Rh-coe bond imparted by the bulky $\eta^6\text{-C}_6\text{H}_5\text{-BPh}_3$ ligand.

Reliable assignment for the ^1H and $^{13}\text{C}\{^1\text{H}\}$ resonances of both rotamers was achieved by combination of the ^1H - ^1H COSY, ^{13}C APT and ^1H - ^{13}C HSQC spectra (see SI). The analysis of the spectroscopic data is in agreement with an equilibrium between the *endo-endo* and *exo-endo* rotamers (Figure 3).

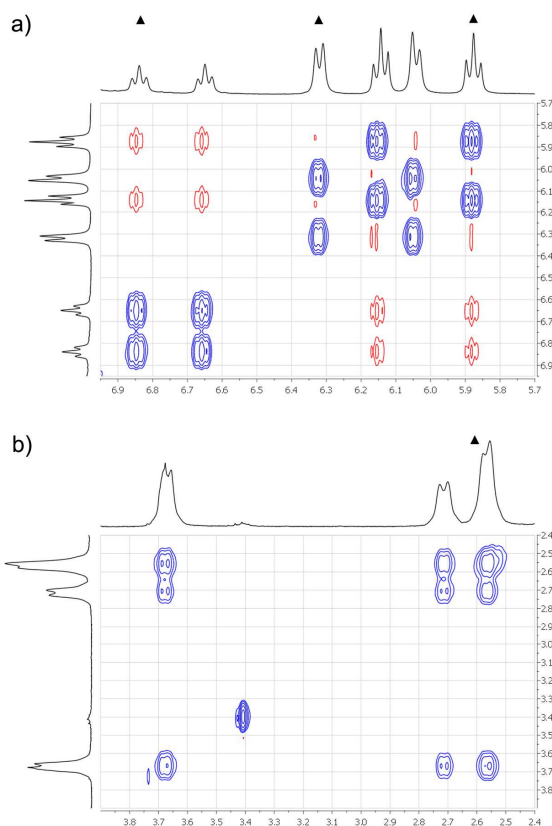


Figure 2. Selected regions of the ^1H - ^1H NOESY NMR spectrum of **1** in CD_2Cl_2 at 253 K: a) $(\eta^6\text{-C}_6\text{H}_5\text{-B})\text{Rh}$ region, b) olefinic $=\text{CH}$ region (▲ *endo-endo* rotamer, unlabeled resonances *exo-endo* rotamer).

The *exo-endo* rotamer displays two distinct resonances for the $=\text{CH}$ protons at 3.62 (*exo*) and 2.68 ppm (*endo*) in the ^1H NMR spectrum, which points to an ideal C_s symmetry, if free rotation of the phenyl rings and a low rotational barrier about the arene-rhodium axis is assumed. Accordingly, two resonances were observed for the $=\text{CH}$ carbons at 74.84 ($J_{\text{C-Rh}} = 13.2$ Hz, *endo*) and 63.02 ppm ($J_{\text{C-Rh}} = 12.0$ Hz, *exo*) in the $^{13}\text{C}\{^1\text{H}\}$ spectrum. In agreement with the ideal C_{2v} symmetry, the *endo-endo* rotamer shows a single resonance at 2.54 ppm for the $=\text{CH}$ protons, however, a broad coalesced resonance at 78.32 ppm was observed for the equivalent olefinic carbons.

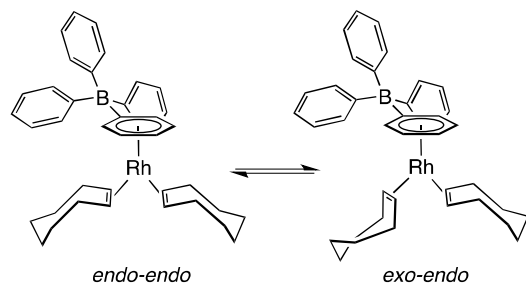


Figure 3. Equilibrium between the *endo-endo* and *exo-endo* rotamers in zwitterionic complexes $[(\eta^6\text{-C}_6\text{H}_5\text{-BPh}_3)\text{M}(\text{coe})_2]$ ($\text{M} = \text{Rh, Ir}$).

Restricted rotation of the cyclooctene ligands was also observed in the analogous iridium compound $[(\eta^6\text{-C}_6\text{H}_5\text{-BPh}_3)\text{Ir}(\text{coe})_2]$ (**2**). Compound **2** was prepared by reaction of the solvato species $[\text{Ir}(\text{coe})_2(\text{Me}_2\text{CO})_x]^+$ with NaBPh_4 in acetone and isolated as a white solid in good yield. The ^1H NMR spectrum of **2** in CD_2Cl_2 showed the presence of the *endo-endo* and *exo-endo* rotamers in a 3:1 ratio. As it was observed for **1**, the $=\text{CH}$ protons of the *coe* ligands for the *exo-endo* rotamer were found to be shifted significantly downfield (3.52 and 2.46 ppm) compared to the *endo-endo* rotamer (2.10 ppm). In the same way, the $=\text{CH}$ carbons were found upfield-shifted for the *exo-endo* rotamer (57.62 and 45.06 ppm). However, in contrast with **1**, this resonance for the *endo-endo* rotamer was observed as a sharp singlet at 62.64 ppm. The molecular structure of the iridium zwitterionic compound **2** has been determined by an X-ray diffraction study. As suggested from the similar cell parameters, complexes **1** and **2** resulted to be isotopic in the solid state. An analogous molecular structure has been found, with minor changes in the structural parameters (see Table 1), most probably associated to small differences in the crystalline disorder.

The Ir-G(centroid) distance (1.806(2) Å) in **2** is similar to that reported in **1**, and again a broad range of Ir-C bond distances (2.233(6)-2.401(5) Å) has been observed. However, it is interesting to remark that these M-C(arene) distances, in both complexes, exhibit an analogous pattern having two significantly shorter distances (2.250 and 2.261(3) Å in **1**, and 2.233(6) and 2.241(5) Å in **2**), and a clearly longer distance for the *ipso* carbon (2.410(3) Å in **1**, and 2.401(5) Å in **2**). The two shortest Rh-C distances are nearly *trans*-disposed to the olefinic bonds, showing the electronic inter-ligand influence through the metal.

Although the olefinic C=C bond distances seems not to be sensitive to the electronic or steric effects, as they exhibit statistically identical values for the two *coe* molecules in both complexes, and similar to the values reported in related systems,²⁴ the M-C(olefin) distances clearly showed a dependence of the *endo/exo* disposition, having shorter M-C bond distances for the *endo* conformations (2.172(3) in **1**, and 2.163(5) Å in **2**) and longer for the *exo* dispositions (2.244(3) in **1**, and 2.198(8) Å in **2**).

The three rotational isomers of complexes $[(\eta^6\text{-C}_6\text{H}_5\text{-BPh}_3)\text{M}(\text{coe})_2]$ ($\text{M} = \text{Rh, Ir}$) have been optimized by DFT calculations using the B3PW91 functional and its relative free energy calculated through frequency analysis. The most stable isomer of the rhodium compound is the *exo-endo*, being the *endo-endo* isomer just at $\Delta G = 2.8$ kJ·mol⁻¹ above it. The *exo-exo* is the less stable isomer by $\Delta G = 32.8$ kJ·mol⁻¹ above the first one. This suggests that only the *exo-endo* and *endo-endo* isomers are close enough in energy to be involved in the observed equilibrium while the *exo-exo* remains unobserved.²⁶ For the iridium compound a similar relationship has been calculated. The highest energy isomer is the *exo-exo* which is at $\Delta G = 41.7$ kJ·mol⁻¹ above the *exo-endo* while the *endo-endo* is just at $\Delta G = 2.0$ kJ·mol⁻¹ above it.

The rotation process between the *exo-endo* and *endo-endo* conformers of the rhodium compound has been studied by a

series of partial optimizations using a z-matrix coordinates setup and driving the dihedral angle which governs the olefin rotation towards +180 and -180° values in 15° steps spanning a full rotation of one of the coe ligands. In this z-matrix coordinate system the *endo-endo* isomer is located at +16° and the more stable *endo-exo* at 185° (Figure 4). The electronic total energy profile shows some irregularities, which reflect the variable environment of the olefin ligand during the rotation process that can lead to diverse steric interactions. The most relevant feature is the location of two different energy maxima which suggest that the easiest isomerization pathway could be an oscillation of the coe ligand (windshield wiper motion) between its two minimum energy positions through the lowest energy barrier (around 46 kJ·mol⁻¹ of electronic energy, interpolated from the rotation scan) instead of completing a full rotation which would imply ca. 23 kJ·mol⁻¹ of additional electronic energy to surmount the highest barrier which should be a less probable event.

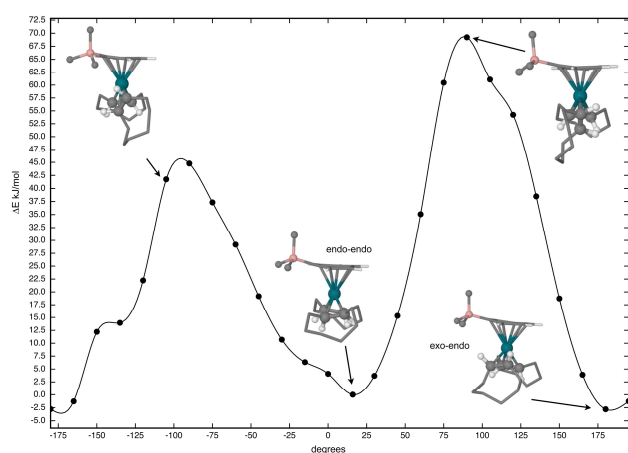


Figure 4. Energy profile for the rotation process interconverting the *endo-endo* and *exo-endo* rotational isomers in complex $[(\eta^6\text{-C}_6\text{H}_5\text{-BPh}_3)\text{Rh}(\text{coe})_2]$ (**1**).

Experimental rotational rates and barriers for **1** and **2** were obtained from magnetization transfer experiments using 2D EXSY NMR spectroscopy. This method has been increasingly applied to the study of complex kinetic processes, fluxional behaviour, rotational barriers and conformational analysis.²⁷ The essential feature of a quantitative 2D EXSY experiment is the relationship between the intensity of the cross-peaks and the rate constants for chemical exchange. The forward and backward exchange rate constants, k_1 and k_{-1} , for the rotamer equilibrium *endo-endo* \rightleftharpoons *exo-endo* in complexes **1** and **2** (Figure 3) were determined by integration of the cross-peaks between the *para* resonances of the η^6 -arene in both interconverting species in the ¹H 2D-EXSY NMR spectrum. The integrals of the exchanged cross-peaks were processed using the EXSYCalc program to give the rate constants (k and k_{-1}),²⁸ and the activation energies by using the Eyring equation (see SI). The kinetic parameters for the *endo-endo* \rightleftharpoons *exo-endo* equilibrium are summarized in Table 2.

The forward and backward exchange rate constants, k_1 and k_{-1} , for the rhodium complex **1** were calculated to be 2.59 s⁻¹ with an associated activation barrier of 64.5 kJ·mol⁻¹ (273 K). However, the iridium complex **2** showed smaller rate constants, 0.016 and 0.051 s⁻¹, and consequently higher activation barriers of 83.81 and 80.91 kJ·mol⁻¹ (300 K). Noteworthy, the calculated

equilibrium constants obtained from the determined rate constants (k_1/k_{-1}) are in good agreement with those experimental values obtained from the same sample by integration of both resonances in an experiment recorded with the same relaxation time.

Table 2. ¹H 2D EXSY-derived rate constants (k_1 and k_{-1}/s^{-1}) and activation energies (ΔG_1^\ddagger and $\Delta G_{-1}^\ddagger/\text{kJ}\cdot\text{mol}^{-1}$) for the *endo-endo* \rightleftharpoons *exo-endo* equilibrium in zwitterionic $[\text{M}(\eta^6\text{-C}_6\text{H}_5\text{-BPh}_3)(\text{coe})_2]$ (M = Rh, Ir) complexes.^a

	t_m (ms)	T_1 (ms)	k_1 (s ⁻¹) ^b	k_{-1} (s ⁻¹) ^b	ΔG_1^\ddagger (kJ·mol ⁻¹) ^c	ΔG_{-1}^\ddagger (kJ·mol ⁻¹) ^c	K = k_1/k_{-1}	K (NMR)
1 (Rh)	600	750	2.594	2.598	64.50	64.49	0.998	0.952
2 (Ir)	700	900	0.016	0.051	83.81	80.91	0.314	0.35

^a 2D EXSY NMR spectra (500 MHz) were recorded at 273 K (**1**) or 300 K (**2**) using saturated CD₂Cl₂ solution of the compounds, t_m optimised mixing time, T_1 longitudinal relaxation time. ^b The integrations for the exchange cross-peaks were processed using the EXSYCalc program to obtain the rate constants k_1 and k_{-1} . ^c Eyring equation was used to calculate activation energies ΔG_1^\ddagger and ΔG_{-1}^\ddagger ; $\Delta G^\ddagger = \square RT \ln(hk/k_B T)$, T is temperature in Kelvin, k_B is the Boltzmann's constant and h is Planck's constant.

Rotation about the M(η^6 -arene) bond axis in zwitterionic $[(\eta^6\text{-C}_6\text{H}_5\text{-BPh}_3)\text{ML}_n]$ complexes is expected to have a low rotational barrier under no steric constraints. In fact, restricted rotation has only been observed in complex $[(\eta^6\text{-C}_6\text{H}_5\text{-BPh}_3)\text{Rh}(\text{dppb})]$ (dppb = 1,4-bis(diphenylphino)butane) down to 194 K.²⁹ Most probably this effect is a consequence of the size of the seven-membered chelate ring that produces steric interference with the phenyl groups of the tetraphenylborate fragment.

To the best of our knowledge, the only examples for which the free energy of activation for the cyclooctene rotation about the metal-cyclooctene bond axis has been determined are complexes $[(\eta^5\text{-C}_9\text{H}_7)\text{Ir}(\text{coe})(\text{CO})]$ and $[(\eta^5\text{-C}_5\text{H}_5)\text{Ir}(\text{coe})(\text{CO})]$, the indenyl complex exhibiting a significantly lower rotational barrier than the corresponding cyclopentadienyl complex, 60.7 and 84.5 kJ·mol⁻¹, respectively.^{22b} Interestingly, the propeller-like ethylene rotation in related complexes $[(\eta^5\text{-C}_9\text{H}_7)\text{Ir}(\text{C}_2\text{H}_4)(\text{CO})]$ and $[(\eta^5\text{-C}_5\text{H}_5)\text{Ir}(\text{C}_2\text{H}_4)(\text{CO})]$ showed comparable rotational barriers of 58.1 and 83.6 kJ·mol⁻¹, respectively.³⁰ As it has been found in our zwitterionic $[(\eta^6\text{-C}_6\text{H}_5\text{-BPh}_3)\text{M}(\text{coe})_2]$ complexes, the ethylene rotation barrier in the Ir(I) complex $[(\eta^5\text{-C}_5\text{H}_5)\text{Ir}(\eta^2\text{-C}_2\text{H}_4)_2]$ is higher than in the Rh(I) complex $[(\eta^5\text{-C}_5\text{H}_5)\text{Rh}(\eta^2\text{-C}_2\text{H}_4)_2]$, 80.6 and 65.6 kJ·mol⁻¹, respectively.³¹

In contrast to $[(\eta^6\text{-C}_6\text{H}_5\text{-BPh}_3)\text{Rh}(\text{diene})]$, the bis-cyclooctene complex $[(\eta^6\text{-C}_6\text{H}_5\text{-BPh}_3)\text{Rh}(\text{coe})_2]$ (**1**) showed no catalytic activity for the polymerization of monosubstituted acetylenes illustrating the key role of the diene ligand in the former efficient initiators. On the other hand, preliminary reactivity studies have shown that replacement reactions on **1** take place quite slowly under thermal conditions suggesting that the cyclooctene ligands are far less labile than previously thought, thereby limiting their application as synthetic precursor when using highly sensitive hemilabile phosphines. As an example, reaction of **1** with two equiv of PPh₃ to give $[(\eta^6\text{-C}_6\text{H}_5\text{-BPh}_3)\text{Rh}(\text{PPh}_3)_2]$ ^{5a} required 1 hour at 333 K in tetrahydrofuran/methanol (3:1) (70% isolated yield).

Conclusions

The zwitterionic $[(\eta^6\text{-C}_6\text{H}_5\text{-BPh}_3)\text{M}(\text{coe})_2]$ ($\text{M} = \text{Rh}, \text{Ir}$) complexes have been prepared from standard cyclooctene starting materials in good yield. The solid-state crystal structures of both complexes show an unusual *exo-endo* disposition of the cyclooctene ligands. In solution, both complexes exhibit an interesting dynamic behaviour associated to the hindered rotation about the metal-cyclooctene bond imparted by the bulky $\eta^6\text{-C}_6\text{H}_5\text{-BPh}_3$ ligand. The equilibrium between the *endo-endo* and *exo-endo* rotational isomers has been fully characterized by means of 2D NMR correlation spectroscopy. Both rotamers were found in 1:1 ratio in the rhodium complexes whereas the *endo-endo* rotamer predominated in the iridium complex (3:1 ratio). DFT calculations in both complexes have shown that the energy of *exo-exo* rotational isomer is well over that of the more stable *endo-endo* isomer. In contrast, the *exo-endo* and *endo-endo* rotational isomers are close enough in energy, which is in full agreement with the observed equilibrium. Average rotational barriers of around $65 \text{ kJ}\cdot\text{mol}^{-1}$ (Rh) and $84 \text{ kJ}\cdot\text{mol}^{-1}$ (Ir) have been determined experimentally by 2D EXSY NMR spectroscopy. The energy profile for the rotation process interconverting the *endo-endo* and *exo-endo* rotational isomers strongly suggests that the most probably isomerization pathway is a windshield wiper motion of the cyclooctene ligands instead of completing a full rotation. Finally, preliminary reactivity studies on these zwitterionic complexes have shown that the cyclooctene ligands are less labile than could be expected.

Experimental

Synthesis

All experiments were carried out under an atmosphere of argon using Schlenk techniques. Solvents were obtained from a Solvent Purification System (Innovative Technologies). Oxygen-free solvents were employed throughout. CD_2Cl_2 was dried using activated molecular sieves. Standard literature procedures were used to prepare the starting materials $[\text{Rh}(\mu\text{-Cl})(\text{coe})_2]_2$ ³² and $[\text{Ir}(\mu\text{-Cl})(\text{coe})_2]_2$.³³

Scientific Equipment

Elemental analyses were carried out in a Perkin-Elmer 2400 CHNS/O analyzer. NMR spectra were recorded on a Bruker Avance 400 spectrometer. ^1H (400.13 MHz) and ^{13}C (100.61 MHz) NMR chemical shifts are reported in ppm relative to tetramethylsilane and referenced to partially deuterated solvent resonances. Coupling constants (J) are given in Hertz. ^1H 2D EXSY NMR spectra were recorded on a Bruker Avance 500 spectrometer operating at 500.13 MHz. Spectral assignments were achieved by combination of ^1H - ^1H COSY, NOESY, ^{13}C DEPT and APT, ^1H - ^{13}C HSQC and ^1H - ^{13}C HMBC experiments. Electrospray mass spectra (ESI-MS) were recorded on a Bruker MicroToF-Q using sodium formate as reference.

$[(\eta^6\text{-C}_6\text{H}_5\text{-BPh}_3)\text{Rh}(\text{coe})_2]$ (1)

NaBPh_4 (210 mg, 0.614 mmol) was added to a yellow suspension

of $[\text{Rh}(\mu\text{-Cl})(\text{coe})_2]_2$ (200.0 mg, 0.279 mmol) in methanol (12 mL). The suspension was stirred for 5 h to give a pale yellow solid which was separated by filtration, washed with methanol (4 x 4 mL) and dried in vacuum. Yield: 92% (330 mg). Anal. Calcd for $\text{C}_{40}\text{H}_{48}\text{BRh}$: C, 74.77; H, 7.53. Found: C, 74.21; H 7.19. Spectroscopic analysis at 253K showed the existence of two rotamers, *endo-endo* (*R1*) and *exo-endo* (*R2*), in 1:1 ratio. ^1H NMR (400.13 MHz, 298 K, CD_2Cl_2): δ 7.45–7.00 (m, 30H, -BPh₃), 6.86, 6.71 (br m, 2H each, H_p), 6.36 (br m, 2H, H_o/H_m), 6.16 (br m, 4H, H_o/H_m), 5.92 (br m, 2H, H_o/H_m) ($\eta^6\text{-C}_6\text{H}_5$), 3.76 (br m, 2H, =CH, coe), 2.83–1.03 (m, 54H, =CH and >CH₂, coe). ^1H NMR (400.13 MHz, 253 K, CD_2Cl_2): δ 7.30 (m, 6H), 7.21 (m, 6H), 7.12 (m, 12H), 7.02 (m, 6H) (-BPh), 6.84 (t, 1H, $J_{\text{H-H}} = 6.1$, H_p, *R1*), 6.65 (t, 1H, $J_{\text{H-H}} = 6.1$ Hz, H_p, *R2*), 6.29 (d, 2H, $J_{\text{H-H}} = 6.1$ Hz, H_o, *R1*), 6.15 (t, 2H, $J_{\text{H-H}} = 6.4$ Hz, H_m, *R2*), 6.00 (d, 2H, $J_{\text{H-H}} = 6.1$ Hz, H_o, *R2*), 5.88 (t, 2H, $J_{\text{H-H}} = 6.4$ Hz, H_m, *R1*) ($\eta^6\text{-C}_6\text{H}_5$), 3.62 (m, 2H, =CH, coe, *R2*), 2.68 (m, 2H, =CH, coe, *R2*), 2.54 (m, 4H, =CH, coe, *R1*), 2.30–1.20 (m, 48H, >CH₂, coe). $^{13}\text{C}\{^1\text{H}\}$ NMR (100.61 MHz, 253 K, CD_2Cl_2): δ 135.84, 126.38, 126.23, 123.57, 123.46 (CH, -BPh), 109.56 (d, $J_{\text{C-Rh}} = 2.7$ Hz, C_o, *R1*), 109.35 (d, $J_{\text{C-Rh}} = 2.6$ Hz, C_o, *R2*), 107.21 (d, $J_{\text{C-Rh}} = 2.0$ Hz, C_p, *R2*), 105.72 (d, $J_{\text{C-Rh}} = 2.0$ Hz, C_p, *R1*), 104.65 (d, $J_{\text{C-Rh}} = 3.3$ Hz, C_m, *R1*), 103.95 (d, $J_{\text{C-Rh}} = 2.7$ Hz, C_m, *R2*) (CH, $\eta^6\text{-C}_6\text{H}_5$), 78.32 (br, =CH, coe, *R1*), 74.84 (d, $J_{\text{C-Rh}} = 13.2$ Hz, =CH, coe, *R2*), 63.02 (d, $J_{\text{C-Rh}} = 12.0$ Hz, =CH coe, *R2*), 31.96, 31.62, 31.77, 29.87, 26.46, 25.95, 25.78, 25.72 (>CH₂, coe). ^{11}B NMR (96.3 MHz, 298 K, CD_2Cl_2): -7.43 (s). MS (ESI+, CH₃OH) m/z : 665.1 $[\text{M} + \text{Na}]^+$, 555.2 $[\text{M} - \text{coe} + \text{Na}]^+$, 455.1 $[\text{M} - \text{C}_6\text{H}_5 - \text{coe}]^+$.

$[(\eta^6\text{-C}_6\text{H}_5\text{-BPh}_3)\text{Ir}(\text{coe})_2]$ (2)

NaBPh_4 (76.4 mg, 0.223 mmol) was added to a solution of the solvato complex $[\text{Ir}(\text{coe})_2(\text{Me}_2\text{CO})_x]^+$ (0.223 mmol) prepared *in situ* by treating $[\text{Ir}(\mu\text{-Cl})(\text{coe})_2]_2$ (100.0 mg, 0.112 mmol) with AgBF_4 (43.4 mg, 0.223 mmol) in acetone (15 mL) for 1 h and filtering off the AgCl formed. The orange solution was stirred for 2 h to give a white suspension that was concentrated to 3 mL and then filtered. The iridium compound was extracted with dichloromethane (3 x 2 mL) and the solution brought to dryness under vacuum. Washing of the residue with methanol (2 x 2 mL) gave the compound as a white solid, which was filtered and dried under vacuum. Yield: 71% (116 mg). Anal. Calcd for $\text{C}_{40}\text{H}_{48}\text{BIr}$: C, 65.65; H, 6.61. Found: C, 65.58; H 6.92. Spectroscopic analysis showed the existence of two rotamers, *endo-endo* (*R1*) and *exo-endo* (*R2*), in 3:1 ratio, respectively. ^1H NMR (400.13 MHz, 298 K, CD_2Cl_2): δ 7.33 (m), 7.27 (m), 7.17 (m), 7.07 (m), (-BPh), 6.74 (t, $J_{\text{H-H}} = 5.9$, H_p, *R1*), 6.59 (t, $J_{\text{H-H}} = 5.9$ Hz, H_p, *R2*), 6.37 (d, $J_{\text{H-H}} = 5.8$ Hz, H_o, *R1*), 6.13 (t, $J_{\text{H-H}} = 6.0$ Hz, H_m, *R2*), 6.05 (d, $J_{\text{H-H}} = 5.8$ Hz, H_o, *R2*), 5.85 (t, $J_{\text{H-H}} = 6.0$ Hz, H_m, *R1*) ($\eta^6\text{-C}_6\text{H}_5$), 3.52 (m, =CH, coe, *R2*), 2.46 (m, =CH, coe, *R2*), 2.10 (m, =CH, coe, *R1*), 1.61–1.12 (m, >CH₂, coe). $^{13}\text{C}\{^1\text{H}\}$ NMR (100.61 MHz, 298 K, CD_2Cl_2): δ 136.43, 126.87, 126.75, 124.16, 124.06 (CH, -BPh), 103.04 (C_o, *R1*), 102.79 (C_o, *R2*), 102.50 (C_p, *R2*), 99.61 (C_p, *R1*), 99.38 (C_m, *R1*), 98.21 (C_m, *R2*) (CH, $\eta^6\text{-C}_6\text{H}_5$), 62.64 (=CH, coe, *R1*), 57.62 (=CH, coe, *R2*), 45.06 (=CH, coe, *R2*), 33.17, 33.02, 32.86, 32.79, 30.40, 26.60, 26.42, 26.37, 26.07 (>CH₂, coe). ^{11}B NMR (96.3 MHz, 298 K, CD_2Cl_2): -7.53 (s). MS (ESI+, CH₃OH) m/z : 1145.3 $[\text{M} + \text{Ir}(\text{coe})_2]^+$, 771.2 $[\text{M} + \text{K}]^+$, 655.2 $[\text{M} - \text{C}_6\text{H}_5]^+$.

Theoretical Calculations

All computations were performed using the Gaussian 09 package.³⁴ The structures of the minima were fully optimized without geometrical constraints and confirmed by frequency calculations. The rotation of the cyclooctene ligand was studied by setting up a z-matrix definition for the molecule and driving the relevant dihedral through a full rotation (see SI). Calculations were carried out using the B3PW91 functional and the basis sets used were: LANL2DZ supplemented with an f function³⁵ and its associated ECP for rhodium and 6-31G** for the rest of atoms.

Crystal Structure Determination

Single crystals for the X-ray diffraction study of **1** and **2** (irregular blocks) were grown by slow diffusion of methanol into concentrate solutions of the compounds in CH₂Cl₂ at 253 K. X-ray diffraction data were collected at 100(2) K on a Bruker APEX DUO CCD diffractometer with graphite-monochromated Mo-K α radiation (λ = 0.71073 Å) using narrow ω rotations (0.3°). Intensities were integrated with SAINT-PLUS program³⁶ and corrected for absorption effects with SADABS.³⁷ The structures were solved by direct methods with SHELXS-97³⁸ and refined, by full matrix least-squares on F^2 , with SHELXL-97.³⁹ Both structures were refined first with isotropic and later with anisotropic displacement parameters for non-H atoms. At this point, ADP's revealed that both crystal structures showed a similar static disorder involving both cyclooctene ligands. Eventually two disordered cyclooctene moieties were included in the refinement with some feeble geometrical restrictions to model each of the two olefins present in the complexes [(η^6 -C₆H₅-BPh₃)M(coe)₂]; in the case of **1** a unique complementary occupancy factor was used for both coe molecules (0.678/0.322(4)), while in the case of **2** each disordered coe was refined with an independent complementary occupancy (0.776/0.224(8) and 0.578/0.422(10)). Eventually only the two most abundant coe molecules allow the refinement with anisotropic displacement parameters, while isotropic thermal parameters were used for the less abundant disordered molecules. An additional partial molecule (0.25 occupancy factor) of a disordered dichloromethane molecule was also present in both crystal structures. This solvent molecule was observed highly disordered and modelled in the best possible way (see supplementary material). Hydrogen atoms (except those of the disordered CH₂Cl₂ solvent) were included for both complexes from calculated positions and refined with positional and displacement riding parameters.

Crystal Data for **1**: C₄₀H₄₈BRh · 0.25 CH₂Cl₂; M = 663.74; yellow block 0.221 × 0.134 × 0.117 mm³; triclinic; $P-1$; a = 8.9933(5), b = 10.5938(6), c = 17.9914(10), α = 79.8632(8), β = 79.6103(7), γ = 84.0189(8)°; Z = 2; V = 1655.02(16) Å³; D_c = 1.332 g/cm³; μ = 0.584 mm⁻¹; min. and max. absorption correction factors 0.8819 and 0.9359; $2\theta_{\max}$ = 60.74°; 19376 reflections collected, 9114 unique (R_{int} = 0.0231); number of data/restraints/parameters 9114/36/550; final GOF 1.035; R_1 = 0.0556 (7824 reflections, $I > 2\sigma(I)$); $wR(F^2)$ = 0.1256 for all data; largest difference peak 1.247 e/Å³, observed in the spatial region of one of the disordered coe molecules. In this complex, also one

of the non-coordinated phenyl groups of the BPh₄⁻ anion showed static disorder; a simple model with two isotropic C₆H₅ groups with identical occupancy were included in the refinement.

Crystal Data for **2**: C₄₀H₄₈BIr · 0.25 CH₂Cl₂; M = 753.03; colorless block 0.273 × 0.221 × 0.176 mm³; triclinic; $P-1$; a = 9.0451(9), b = 10.6166(10), c = 18.0547(17), α = 78.6882(12), β = 79.8650(13), γ = 83.4888(11)°; Z = 2; V = 1668.0(3) Å³; D_c = 1.499 g/cm³; μ = 4.070 mm⁻¹; min. and max. absorption correction factors 0.4029 and 0.5345; $2\theta_{\max}$ = 58.14°; 17480 reflections collected, 8303 unique (R_{int} = 0.0204); number of data/restraints/parameters 8303/38/473; final GOF 1.158; R_1 = 0.0458 (7570 reflections, $I > 2\sigma(I)$); $wR(F^2)$ = 0.1116 for all data; largest difference peak 3.327 e/Å³. Five residuals over 1 e/Å³ were observed in the final Fourier map; the three more intense were in close proximity to the metal (with no chemical sense) and the two additional in the region of the disordered coe molecules.

Acknowledgments

Financial support from the Spanish Ministerio de Economía y Competitividad (MINECO/FEDER) of Spain (CTQ2010-15221 and CONSOLIDER INGENIO CSD2009-00050), the Diputación General de Aragón (DGA/FSE-E07) and the ARAID Foundation, is gratefully acknowledged.

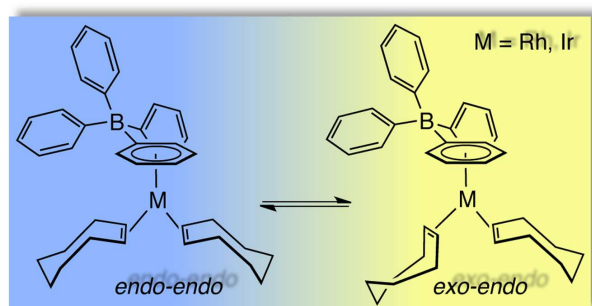
Notes and references

- ^a Departamento de Química Inorgánica, Instituto de Síntesis Química y Catálisis Homogénea-ISQCH, Universidad de Zaragoza-CSIC, Facultad de Ciencias, C/ Pedro Cerbuna, 12, 50009 Zaragoza, Spain. Fax: 34 976761143; Tel: 34 976762025; E-mail: perez@unizar.es
- [§] ARAID Foundation researcher
- [†] Electronic Supplementary Information (ESI) available: NMR spectra and experimental procedure for the determination of the kinetic parameters by 2D-EXSY spectroscopy. Computed cartesian coordinates of all of the molecules reported in this study (MCOE.xyz file) and z-matrix setup used as starting point in the study of the rotation of the coe ligand in **1** (RhCOE.zmat file). See DOI: 10.1039/b000000x/
- [‡] CCDC numbers 1013126-1013127.
- a) M. Stradiotto, K. D. Hesp, R. J. Lundgren, *Angew. Chem. Int. Ed.*, 2010, **49**, 494–512; b) R. Chauvin, *Eur. J. Inorg. Chem.* 2000, 577–591.
- a) E. -E. Bendeif, C. F. Matta, M. Stradiotto, P. Fertey, C. Lecomte, *Inorg. Chem.*, 2012, **51**, 3754–3769; b) Z. -J. Yao, X. -K. Huo, G.-X. Jin, *Chem. Commun.*, 2012, **48**, 6714–6716.
- I. Krossing, I. Raabe, *Angew. Chem. Int. Ed.*, 2004, **43**, 2066–2090.
- a) A. B. Chaplin, A. S. Weller, *Eur. J. Inorg. Chem.*, 2010, 5124–5128; b) G. B. Deacon, D. J. Evans, C. M. Forsyth, P. C. Junk, *Coord. Chem. Rev.*, 2007, **251**, 1699–1706; c) T. M. Douglas, E. Molinos, S. K. Brayshaw, A. S. Weller, *Organometallics*, 2007, **26**, 463–465; d) S. H. Strauss, *Chem. Rev.* 1993, **93**, 927–942.
- a) E. P. Shestakova, Y. S. Varshavsky, V. N. Khrustalev, I. S. Podkorytov, *J. Organomet. Chem.*, 2007, **692**, 4297–4302; b) L. A. Oro, J. V. Heras, K. H. A. Ostojá-Starzewski, A. Heinz, P. S. Pregosin, A. Manrique, M. Royo, *Trans. Met. Chem.*, 1981, **6**, 1–3; c) P. R. Brookes, *J. Organomet. Chem.* 1972, **43**, 415–23.
- a) R. Uson, P. Lahuerta, J. Reyes, L. A. Oro, C. Foces-Foces, F. H. Cano, S. García-Blanco, *Inorg. Chim. Acta*, 1980, **42**, 75–84; b) R. Uson, P. Lahuerta, J. Reyes, L. A. Oro, *Trans. Met. Chem.*, 1979, **4**, 332–333; c) L. M. Haines, *Inorg. Chem.* 1971, **10**, 1685–1692.
- M. Aresta, E. Quaranta, A. Albinati, *Organometallics*, 1993, **12**, 2032–2043.

- 8 a) L. A. Oro, E. Pinilla, M. L. Tenajas, *J. Organomet. Chem.*, 1978, **148**, 81–84; b) R. R. Schrock, J. A. Osborn, *Inorg. Chem.*, 1970, **9**, 2339–2343.
- 9 a) B. Longato, G. Pilloni, R. Graziani, U. Casellato, *J. Organomet. Chem.*, 1991, **407**, 369–376; b) E. G. Thaler, K. G. Caulton, *Organometallics*, 1990, **9**, 1871–1876; c) J. M. Brown, P. A. Chaloner, A. G. Kent, B. A. Murrer, P. N. Nicholson, D. Parker, P. J. Sidebottom, *J. Organomet. Chem.*, 1981, **216**, 263–76. d) P. Albano, M. Aresta, M. Manassero, *Inorg. Chem.*, 1980, **19**, 1069–1072.
- 10 a) M. Aresta, E. Quaranta, *J. Organomet. Chem.*, 1993, **463**, 215–221; b) G. Mestroni, G. Zassinovich, A. Camus, *J. Organomet. Chem.*, 1977, **140**, 63–72.
- 11 a) B. G. van den Hoven, H. Alper, *J. Am. Chem. Soc.* 2001, **123**, 10214–10220. b) Y. -S. Lin, B. El Ali, H. Alper, *J. Am. Chem. Soc.*, 2001, **123**, 7719–7720; c) Z. Zhou, G. Facey, B. R. James, H. Alper, *Organometallics*, 1996, **15**, 2496–2503 (and references therein).
- 12 a) R. Shintani, Y. -T. Soh, T. Hayashi, *Org. Lett.*, 2010, **12**, 4106–4109; b) R. Shintani, Y. Tsutsumi, M. Nagaosa, T. Nishimura, T. Hayashi, *J. Am. Chem. Soc.*, 2009, **131**, 13588–13589.
- 13 a) T. Masuda, *J. Polym. Sci., Part A: Polym. Chem.*, 2007, **45**, 165–180; b) M. G. Mayershofer, O. Nuyken, *J. Polym. Sci., Part A: Polym. Chem.*, 2005, **43**, 5723–5747.
- 14 I. Saeed, M. Shiotsuki, T. Masuda, *Macromolecules*, 2006, **39**, 8977–8981.
- 15 a) Y. Ichikawa, T. Nishimura, T. Hayashi, *Organometallics*, 2011, **30**, 2342–2348; b) N. Onishi, M. Shiotsuki, F. Sanda, T. Masuda, *Macromolecules*, 2009, **42**, 4071–4076; c) T. Nishimura, Y. Ichikawa, T. Hayashi, N. Onishi, M. Shiotsuki, T. Masuda, *Organometallics*, 2009, **28**, 4890–4893; d) Y. Kishimoto, M. Itou, T. Miyatake, T. Ikariya, R. Noyori, *Macromolecules*, 1995, **28**, 6662–6666.
- 16 a) M. V. Jiménez, J. Fernández-Tornos, J. J. Pérez-Torrente, F. J. Modrego, S. Winterle, C. Cunchillos, F. J. Lahoz, L. A. Oro, *Organometallics*, 2011, **30**, 5493–5508; b) M. V. Jiménez, J. J. Pérez-Torrente, M. I. Bartolomé, L. A. Oro, *Synthesis*, 2009, 1916–1922; c) M. V. Jiménez, J. J. Pérez-Torrente, M. I. Bartolomé, V. Gierz, F. J. Lahoz, L. A. Oro, *Organometallics*, 2008, **27**, 224–234.
- 17 a) M. Angoy, M. I. Bartolomé, E. Vispe, P. Lebeda, M. V. Jiménez, J. J. Pérez-Torrente, S. Collins, S. Podzimek, *Macromolecules*, 2010, **43**, 6278–6283. b) M. V. Jiménez, J. J. Pérez-Torrente, M. I. Bartolomé, E. Vispe, F. J. Lahoz, L. A. Oro, *Macromolecules*, 2009, **42**, 8146–8156.
- 18 a) Jiménez, M. V., Bartolomé, M. I., Pérez-Torrente, J. J., Gómez, D., Modrego, F. J., Oro, L. A. *ChemCatChem*, 2013, **5**, 263–276; b) Jiménez, M. V., Bartolomé, M. I., Pérez-Torrente, J. J., Lahoz, F. J., Oro, L. A. *ChemCatChem*, 2012, **4**, 1298–1310; c) Jiménez, M. V., Pérez-Torrente, J. J., Bartolomé, M. I., Lahoz, F. J., Oro, L. A., *Chem. Commun.*, 2010, **46**, 5322–5324.
- 19 L. Palacios, A. Di Giuseppe, A. Opalinska, R. Castarlenas, J. J. Pérez-Torrente, F. J. Lahoz, L. A. Oro, *Organometallics*, 2013, **32**, 2768–2774.
- 20 a) J. W. Faller. *Stereochemical nonrigidity of organometallic complexes*. In *Encyclopedia of Inorganic Chemistry*, R. B. King, Ed.; Wiley: New York; 1994, Vol. 7, p. 3914–3933; b) B. E. Mann, *Non-rigidity in Organometallic Compounds*. In *Comprehensive Organometallic Chemistry*; G. Wilkinson, F. G. A. Stone, E. W. Abel, Eds.; Pergamon Press: New York; 1982, Vol. 3, Chapter 20, pp 89–168; c) R. Benn, *Org. Magn. Reson.*, 1983, **21**, 723–726; d) T. A. Albright, R. Hoffmann, J. C. Thibeault, D. L. Thorn, *J. Am. Chem. Soc.*, 1979, **101**, 3801–3812; d) R. Cramer, *J. Am. Chem. Soc.*, 1964, **86**, 217–222.
- 21 a) A. Di Giuseppe, R. Castarlenas, J. J. Pérez-Torrente, M. Crucianelli, V. Polo, R. Sancho, F. J. Lahoz, L. A. Oro, *J. Am. Chem. Soc.*, 2012, **134**, 8171–8183; b) L. Palacios, X. Miao, A. Di Giuseppe, S. Pascal, C. Cunchillos, R. Castarlenas, J. J. Pérez-Torrente, F. J. Lahoz, P. H. Dixneuf, L. A. Oro, *Organometallics*, 2011, **30**, 5208–5213; c) P. J. Albietz, B. P. Cleary, W. Paw, R. Eisenberg, *Inorg. Chem.*, 2002, **41**, 2095–2108; d) J. L. McBee, J. Escalada, T. D. Tilley, *J. Am. Chem. Soc.*, 2009, **131**, 12703–12713; e) E. B. Wickeneiser, W. R. Cullen, *Inorg. Chem.*, 1990, **29**, 4671–4676; f) M. Mlekuz, P. Bougeard, B. G. Sayer, M. J. McGlinchey, C. A. Rodger, M. R. Churchill, J. W. Ziller, S.-K. Kang, T. A. Albright *Organometallics*, 1986, **5**, 1656–1663.
- 22 a) A. Friedrich, R. Ghosh, R. Kolb, E. Herdtweck, S. Schneider, *Organometallics*, 2009, **28**, 708–718; b) L. P. Szajek, J. R. Shapley, *Organometallics*, 1994, **13**, 1395–1403.
- 23 a) M. J. Geier, C. M. Vogels, A. Decken, S. A. Westcott, *Eur. J. Inorg. Chem.*, 2010, 4602–4610; b) C. Y. Tang, W. Smith, D. Vidovic, A. L. Thompson, A. B. Chaplin, S. Aldridge, *Organometallics*, 2009, **28**, 3059–3066; c) T. Yamagata, K. Nakajima, K. Arimitsu, A. Iseki, K. Tani, *Acta Crystallogr., Sect. E: Struct. Rep. Online*, 2008, **64**, m579–m580; d) W.-M. Cheung, C.-Y. Lai, Q.-F. Zhang, W. Y. Wong, I. D. Williams, W.-H. Leung, *Inorg. Chim. Acta*, 2006, **359**, 2712–2720; e) J. M. Burke, R. B. Coapes, A. E. Goeta, J. A. K. Howard, T. B. Marder, E. G. Robins, S. A. Westcott, *J. Organomet. Chem.*, 2002, **649**, 199–203; f) L. Dahlenburg, M. Kuhnlein, *Acta Crystallogr., Sect. C: Cryst. Struct. Commun.*, 2001, **57**, 709–710; g) H. Werner, M. E. Schneider, M. Bosch, J. Wolf, J. H. Teuben, A. Meetsma, S. I. Troyanov, *Chem. Eur. J.*, 2000, **6**, 3052–3059.
- 24 a) C. N. Garon, D. I. McIsaac, C. M. Vogels, A. Decken, I. D. Williams, C. Kleeberg, T. B. Marder, S. A. Westcott, *Dalton Trans.*, 2009, 1624–1631; b) J. S. Siegel, K. K. Baldrige, A. Linden, R. Dorta, *J. Am. Chem. Soc.*, 2006, **128**, 10644–10645; c) P. C. McGowan, C. E. Hart, B. Donnadieu, R. Poilblanc, *J. Organomet. Chem.*, 1997, **528**, 191–194.
- 25 N. Nebra, N. Saffon, L. Maron, B. Martin-Vaca, D. Bourissou, *Inorg. Chem.*, 2011, **50**, 6378–6386.
- 26 Although the tiny resonance at δ 3.41 ppm in the ^1H NMR spectrum of **1** could be tentatively assigned to the *exo-exo* rotational isomer, we do not have conclusive evidence as neither exchange cross peaks (^1H - ^1H NOESY) nor correlation (^1H - ^{13}C HSQC) could be observed in the NMR spectra (see SI).
- 27 a) M. V. Jiménez, F. J. Lahoz, L. Lukešová, J. R. Miranda, F. J. Modrego, D. H. Nguyen, L. A. Oro, J. J. Pérez-Torrente, *Chem. Eur. J.*, 2011, **17**, 8115–8128; b) K. Nikitin, H. Müller-Bunz, Y. Ortin, J. Muldoon, M. J. McGlinchey, *J. Am. Chem. Soc.*, 2010, **132**, 17617–17622; c) T. Amaya, H. Sakane, T. Muneishi, T. Hirao, *Chem. Commun.*, 2008, 765–767; d) D. Carmichael, L. Ricard, N. Seeboth, J. M. Brown, T. D. W. Claridge, B. Odell, *Dalton Trans.*, 2005, 2173–2181; e) F. P. Cossío, P. de la Cruz, A. de la Hoz, F. Langa, N. Martín, P. Prieto, L. Sánchez, *Eur. J. Org. Chem.*, 2000, 2407–2415.
- 28 Cross-peaks were integrated and processed with the EXSYCalc software distributed by Mestrelab Research (<http://mestrelab.com/>).
- 29 Z. Zhou, G. Facey, B. R. James, H. Alper, *Organometallics*, 1996, **15**, 2496–2503.
- 30 L. P. Szajek, R. J. Lawson, J. R. Shapley, *Organometallics*, 1991, **10**, 357–361.
- 31 a) H. Eshtiagh-Hosseini, J. F. Nixon, *J. Less-Common Met.*, 1978, **61**, 107–121, b) R. Cramer, J. B. Kline, J. D. Roberts, *J. Am. Chem. Soc.*, 1969, **91**, 2519–2524.
- 32 M. A. Bennett, J. D. Saxby, *Inorg. Chem.* 1968, **7**, 321–324.
- 33 M. A. Arthurs, J. Bickerton, S. R. Stobart, J. Wang, *Organometallics* 1998, **17**, 2743–2750.
- 34 M. J. Frisch, G. W. Trucks, H. B. Schlegel, G. E. Scuseria, M. A. Robb, J. R. Cheeseman, G. Scalmani, V. Barone, B. Mennucci, G. A. Petersson, H. Nakatsuji, M. Caricato, X. Li, H. P. Hratchian, A. F. Izmaylov, J. Bloino, G. Zheng, J. L. Sonnenberg, M. Hada, M. Ehara, K. Toyota, R. Fukuda, J. Hasegawa, M. Ishida, T. Nakajima, Y. Honda, O. Kitao, H. Nakai, T. Vreven, J. A. Montgomery, Jr., J. E. Peralta, F. Ogliaro, M. Bearpark, J. J. Heyd, E. Brothers, K. N. Kudin, V. N. Staroverov, R. Kobayashi, J. Normand, K. Raghavachari, A. Rendell, J. C. Burant, S. S. Iyengar, J. Tomasi, M. Cossi, N. Rega, J. M. Millam, M. Klene, J. E. Knox, J. B. Cross, V.

- Bakken, C. Adamo, J. Jaramillo, R. Gomperts, R. E. Stratmann, O. Yazyev, A. J. Austin, R. Cammi, C. Pomelli, J. W. Ochterski, R. L. Martin, K. Morokuma, V. G. Zakrzewski, G. A. Voth, P. Salvador, J. J. Dannenberg, S. Dapprich, A. D. Daniels, Ö. Farkas, J. B. Foresman, J. V. Ortiz, J. Cioslowski, D. J. Fox, Gaussian 09, Revision B.01 2009.
- 35 A. Ehlers, M. Böhme, S. Dapprich, A. Gobbi, A. Höllwarth, V. Jonas, K. Köhler, R. Stegmann, A. Veldkamp, G. Frenking, *Chem. Phys. Lett.*, 1993, **208**, 111–114.
- 36 SAINT-PLUS, version 6.01, 2001, Bruker AXS, Inc, Madison, USA.
- 37 G. M. Sheldrick, SADABS, 1999, University of Göttingen, Göttingen, Germany.
- 38 a) G. M. Sheldrick, *Acta Crystallogr.*, 1990, **A46**, 467–473, b) G. M. Sheldrick, *Methods Enzymol.*, 1997, **276**, 628–641.
- 39 G. M. Sheldrick, *Acta Crystallogr.*, 2008, **A64**, 112–122.

Graphical abstract



Synthesis and Dynamic Behaviour of Zwitterionic $[\text{M}(\eta^6\text{-C}_6\text{H}_5\text{-BPh}_3)(\text{coe})_2]$ ($\text{M} = \text{Rh}, \text{Ir}$) Cyclooctene Complexes

Jesús J. Pérez-Torrente,* Marta Angoy, Daniel Gómez-Bautista, Adrián Palacios, M. Victoria Jiménez, F. Javier Modrego, Ricardo Castarlenas, Fernando J. Lahoz and Luis A. Oro

The zwitterionic $[(\eta^6\text{-C}_6\text{H}_5\text{-BPh}_3)\text{M}(\text{coe})_2]$ ($\text{M} = \text{Rh}, \text{Ir}$) cyclooctene complexes show an unusual equilibrium between the *endo-endo* and *exo-endo* rotational isomers arising from the hindered rotation about the metal-cyclooctene bond.